Journal for ImmunoTherapy of Cancer

Enhanced mutanome analysis towards the induction of neoepitope-reactive T-cell responses for personalized immunotherapy of pancreatic cancer

Michael Volkmar,[1,2] Dana Hoser,[3,4] Claudia Lauenstein,[2] Janina Rebmann,[1] Agnes Hotz-Wagenblatt,[5] Jan Rieger,[2] Isabel Poschke ,[1,2] Jonas P Becker,[6] Angelika B Riemer,[6] Martin Sprick,[7] Andreas Trumpp,[7] Oliver Strobel,[1] Thomas Blankenstein,[8] Gerald Willimsky ,[3,4] Rienk Offringa [1,2]

To cite: Volkmar M, Hoser D, Lauenstein C, *et al*. Enhanced mutanome analysis towards the induction of neoepitope-reactive T-cell responses for personalized immunotherapy of pancreatic cancer. *Journal for ImmunoTherapy of Cancer* 2025;**13**:e011802. doi:10.1136/jitc-2025-011802

► Additional supplemental material is published online only. To view, please visit the journal online (https://doi.org/10.1136/jitc-2025-011802).

MV and DH contributed equally.
GW and RO contributed equally.

Accepted 12 May 2025

For numbered affiliations see end of article.

Correspondence to
Professor Rienk Offringa;
r.offringa@dkfz.de

ABSTRACT

Background Personalized immunotherapy of pancreatic ductal adenocarcinoma (PDAC) through T-cell mediated targeting of tumor-specific, mutanome-encoded neoepitopes may offer new opportunities to combat this disease, in particular by countering recurrence after primary tumor resection. However, the sensitive and accurate calling of somatic mutations in PDAC tissue samples is compromised by the low tumor cell content. Moreover, the repertoire of immunogenic neoepitopes in PDAC is limited due to the low mutational load of the majority of these tumors.

Methods We developed a workflow involving the combined analysis of next-generation DNA and RNA sequencing data from matched pairs of primary tumor samples and patient-derived xenograft models towards the enhanced detection of driver mutations as well as single nucleotide variants encoding potentially immunogenic T-cell neoepitopes. Subsequently, we immunized HLA/human T-cell receptor (TCR) locus-transgenic mice with synthetic peptides representing candidate neoepitopes, and molecularly cloned the genes encoding TCRs targeting these epitopes.

Result Application of our pipeline resulted in the identification of greater numbers of non-synonymous mutations encoding candidate neoepitopes with increased confidence. Furthermore, we provide proof of concept for the successful isolation of HLA-restricted TCRs from humanized mice immunized with different neoepitopes, several of which would not have been selected based on mutanome analysis of PDAC tissue samples alone. These TCRs mediate specific T-cell reactivity against the tumor cells in which the corresponding mutations were identified.

Conclusion Enhanced mutanome analysis and candidate neoepitope selection increase the likelihood of identifying therapeutically relevant neoepitopes, and thereby support the optimization of personalized immunotherapy for PDAC and other poorly immunogenic cancers.

WHAT IS ALREADY KNOWN ON THIS TOPIC

⇒ Personalized T-cell therapy through targeting of mutanome-encoded neoepitopes is emerging as a promising strategy for the treatment of pancreatic ductal adenocarcinoma (PDAC). However, accurate and sensitive identification of neo-epitopes in PDAC is hampered by the high stromal content of human tumor samples.

WHAT THIS STUDY ADDS

⇒ Here, we demonstrate that mutanome analysis in matched pairs of patient derived xenograft (PDX) models and primary tumor samples facilitates the identification of neoepitopes in PDAC against which T-cell receptors can be generated that mediate epitope-specific, HLA-restricted antitumor T-cell immunity.

HOW THIS STUDY MIGHT AFFECT RESEARCH, PRACTICE OR POLICY

⇒ Only a fraction of predicted neoepitopes is actually presented at the tumor cell surface. However, peptides that do not represent natural T-cell epitopes can be immunogenic and elicit T-cell immunity. Our pipeline for enhanced mutanome analysis and neoepitope prediction increases the likelihood that candidate neoepitope selection results in the identification of therapeutically relevant target antigens.

INTRODUCTION

Pancreatic ductal adenocarcinoma (PDAC), the most common type of pancreatic cancer, has long been regarded as an immunologically "cold" tumor not amenable to T-cell mediated immunotherapy. These tumors are generally unresponsive to immune checkpoint blockade, due to the immunosuppressive tumor microenvironment (TME) and low mutational load, which limits T-cell immunity through mutanome-encoded neoepitopes.[1–3] Nevertheless, an increasing number of studies have revealed the existence of a tumor-reactive T-cell infiltrate in PDAC, as well as the potential relevance of neoepitopes in T-cell-mediated tumor recognition.[4–14] Further

evidence for a natural tumor-reactive T-cell repertoire in human PDAC was recently provided by two complementary studies involving single-cell RNA-sequencing of the CD3+tumor-infiltrating lymphocyte (TIL) repertoire.[15 16] The study by Zheng *et al* focused on the identification of T-cell receptors (TCRs) reactive against neoepitopes as predicted by means of tumor mutanome analysis and HLA-peptide binding algorithms, whereas our own study by Meng *et al* involved an orthogonal, epitope-agnostic approach focusing on the identification of TCRs reactive against autologous tumor cell cultures. In both studies, the corresponding TCR clonotypes were enriched in T cells displaying an exhausted transcriptional state, bearing witness to the encounter of their cognate antigen in the TME. This sets them apart from pathogen-reactive bystander TCR clonotypes that dominate the T-cell infiltrate in PDAC tumors.[15]

A key difference between these studies is that our analyses did not reveal reactivity against predicted mutanome-encoded neoepitopes, suggesting that these may not represent the immunodominant antigens as targeted by the natural T-cell response against PDAC,[15] whereas the study by Zheng *et al* did not include testing of TCRs against autologous tumor cells.[16] The latter also applies to a recent clinical study involving personalized neoepitope vaccination of patients with PDAC. Although showing promising outcome with respect to clinical parameters, the question of whether the vaccine-induced, neoepitope-specific T cells would be reactive against tumor cells expressing the relevant epitopes was not addressed,[17] unlike in similar studies performed in metastatic melanoma.[18 19] Notably, only a small fraction of the theoretical immunopeptidome represents naturally processed, HLA-restricted peptide antigens.[20–25] Strongly HLA-binding peptides that do not represent naturally processed epitopes are likely to be immunogenic, as these represent truly foreign antigens. However, T-cell responses induced against such peptides as induced by repeated immunization with synthetic vaccines lack therapeutic relevance, underlining the importance of immunizing with epitopes that are actually presented at the tumor cell surface.[21 23 25 26] In view of the growing interest in the development of personalized T-cell therapy for PDAC, either through neoepitope vaccination or engineered T-cell therapy,[17 27] we therefore embarked on a proof of concept study aimed at the isolation of TCRs targeting neoepitopes as identified by "reverse immunology" in human PDAC tumor samples, the key question being whether these TCRs would mediate T-cell reactivity against autologous tumor cells derived from the same samples.

A significant hurdle for accurate mutanome-based selection of candidate neoepitopes in PDAC is the low tumor cell content of primary tumor samples due to a heavily expanded stromal compartment rich in, among others, cancer-associated fibroblasts and myeloid cells.[2 3] Consequently, a major fraction of the next generation sequencing (NGS) reads as obtained from human tumor samples are derived from non-transformed, stromal cells. This decreases the mutanome sequencing depth at the DNA level, causing mutations to be detected with low mutated allele frequencies (MAF) or even missed.[28 29] Furthermore, this complicates the assessment of the mutated alleles at the RNA level. In order to enable T-cell epitope prediction on the basis of accurate mutanome data, we established a workflow that involves the parallel analysis of exome and transcriptome data from primary human tumors as well as from corresponding patient derived xenograft (PDX) models. Whereas the PDX models also contain stromal cells, these are of mouse origin. The mouse-derived reads can be identified and excluded by means of suitable bioinformatic tools, resulting in PDX-derived DNA sequencing (DNA-seq) and RNA sequencing (RNA-seq) data sets that exclusively comprise reads from the human tumor cells. Our present study shows that this procedure increases the sensitivity and confidence of mutation calling as well as of subsequent neoepitope prediction. For several of the candidate epitopes, which we carefully selected based on further criteria, we successfully generated TCRs, through immunization of HLA-transgenic mice that express a fully human TCR repertoire.[30] Engineered T cells transduced with these TCRs duly recognized the human tumor cells in which the neoepitope-encoding mutations were identified.

MATERIALS AND METHODS

Patient samples and experiments in mice

Samples from 15 patients with primary resectable PDAC were collected for this study on the basis of informed written consent. All samples were anonymized. The only information provided with the sample was the diagnosis "primary resectable PDAC". Freshly resected tumor tissue was obtained through the European Pancreas Center of Heidelberg University Hospital and processed within 1 hour after resection. A representative slice from the center of each PDAC sample was fresh-frozen for histopathological verification of tumor pathology and tumor cell content. Primary xenografts were established as described by us previously.[31] Establishment of PDX models was performed in the central animal facility of the German Cancer Research Center in Heidelberg. Immunization experiments in HLA-A2, TCR locus transgenic mice were performed in the animal facilities of Charité University Berlin. Animal care and all experimental procedures followed the German legal regulations and were approved on the basis of detailed experimental proposals by the governmental review board of the state of Baden-Wuerttemberg, Germany (project numbers G222/15 and G232/20 concerning PDX models) and by the governmental review board of Berlin (project numbers H0086/16 and H0050/21 concerning immunization experiments in humanized mice).

Further materials and methods

See online supplemental materials and methods.

RESULTS

Development and validation of a pipeline for accurate and sensitive mutanome analysis of PDAC tumors

In order to improve mutanome analysis and subsequent neoepitope prediction for human PDAC tumors, we developed the workflow as shown in figure 1a, which involves parallel analysis of the NGS data from matching pairs of primary tumor and PDX samples, followed by systematic comparison of the outcomes. The standard human reference genome (GRCh37/hg19) was employed for mapping of germline and primary tumor exomes. The PDX samples, although enriched in human tumor cells, contain a significant stromal component of mouse origin. We therefore constructed a customized hybrid reference genome that allows distinction between the human-derived and mouse-derived sequence reads, as well as between single nucleotide variants (SNVs) representing somatic mutations in the human tumor cells and SNVs representing mouse/human genetic differences. This encompasses the human chromosomes as well as a murine C57BL/6J reference genome (GRCm38/mm10), which we adapted to comprise the single nucleotide polymorphisms (SNPs) of the NOD/ShiLtJ mouse strain.[32] The latter is critical, because the PDX tumors are routinely propagated in NOD scid gamma (NSG) mice, which are derived from the NOD/ShiLtJ strain. The polymorphisms between C57BL/6J and NOD/ShiLtJ mice comprise over 4 million SNPs that otherwise could be mistaken for mutations in the human tumor cells.

The resulting workflow was applied to a set of fifteen matched NGS dataset pairs (online supplemental table S1). A significant fraction of the tumors included in our study (8/15) were positive for HLA-A*02:01 to facilitate downstream analysis of T-cell mediated recognition of candidate neoepitopes. As shown in figure 1b,c, our hybrid reference genome efficiently eliminated reads from mouse stromal cells that contain inter-species SNPs. We verified that this also applies to reads mapping to highly conserved regions of the exome, as illustrated by the analysis of a 400 bp region encompassing exons 6 and 7 of the *SMAD4* tumor suppressor gene. For four of the tumor samples, immunohistochemistry analysis suggested that the tumor cells were negative for SMAD4. Paradoxically, exome sequencing data from the primary tumor samples showed many *SMAD4* reads, and the same applied to exome data from the PDX samples when analyzed with the human reference genome (figure 1e,f, online supplemental figure S1). Importantly, analysis of PDX exome data with the hybrid reference genome revealed that these reads were derived from the SMAD4-positive, mouse-derived tumor stroma, thereby eliminating the majority of these reads from the exome data set (figure 1g, online supplemental figure S1). This showed that the tumor cells were indeed SMAD4-deficient, in line with the IHC data, and that the failure to detect SMAD4-deletion in the primary human tumor samples was due to wild type reads of stromal origin. Notably, small numbers of mouse reads may still be mismapped to the human genome when they fall entirely within regions with 100% inter-species conservation, such as the major part of SMAD4 exon 7 (figure 1g, online supplemental figure S1). Genome-wide evaluation revealed 385 further highly-to-completely homologous regions, together spanning approximately 53 kb (0.1% of exome), where read mismapping could be detected, but in none of the cases this resulted in critical loss of sensitivity with respect to the detection of somatic mutations (online supplemental figures S2 and S3 and table S2).

We also considered that our pipeline may erroneously call SNVs due to mouse polymorphisms not included in the hybrid reference genome. Indeed, our initial analysis of the 15 PDX samples resulted in the detection of 10 recurrent SNVs other than activating *KRAS* mutations (online supplemental figure S4 and table S3). Scrutiny of these sequences in different mouse strains confirmed that these SNVs represented either polymorphisms between the NOD/ShiLtJ reference genome and the NSG strain used for our PDX models (online supplemental figure S5a,c,d,e), or the absence of the relevant sequences from the NOD/ShiLtJ reference genome (online supplemental figure S5b,f). We therefore assembled a blacklist to exclude these SNVs from further analyses.

The hybrid reference genome enables enhanced detection of somatic mutations

Subsequent application of our hybrid reference genome towards identification of non-synonymous SNVs (nsSNVs) in our PDX tumor panel resulted in mutation calling with higher sensitivity and confidence than analysis of primary tumor exomes. The MAF of mutations shared by PDX and primary tumor is four to five times higher in the majority of PDX samples (figure 2a–c; see online supplemental figure S6 for data from all 15 tumors). As a result, these mutations are detected with higher confidence, not only because of the higher MAF, but also because of greater numbers of mutation-supporting NGS reads. Furthermore, the MAF values as detected in PDX datasets provide an accurate reflection of the fraction of tumor cells harboring these mutations, which is an important aspect of neoepitope selection for T-cell-mediated targeting of cancers. Lastly, the MAF values for most of these shared mutations increase proportionally (online supplemental table S4), supporting the notion that the PDX models constitute a good representation of the corresponding primary tumor.[31] Analysis of the PDX data overall resulted the identification of greater numbers of mutations (figure 2d,e). Mutations detected exclusively in the PDX models most likely were missed in the primary tumor due to the dilution of tumor cell-derived reads by stromal cell-derived reads. Accordingly, multiple PDX-unique mutations could be retraced in the exome data of the corresponding primary tumor, although at

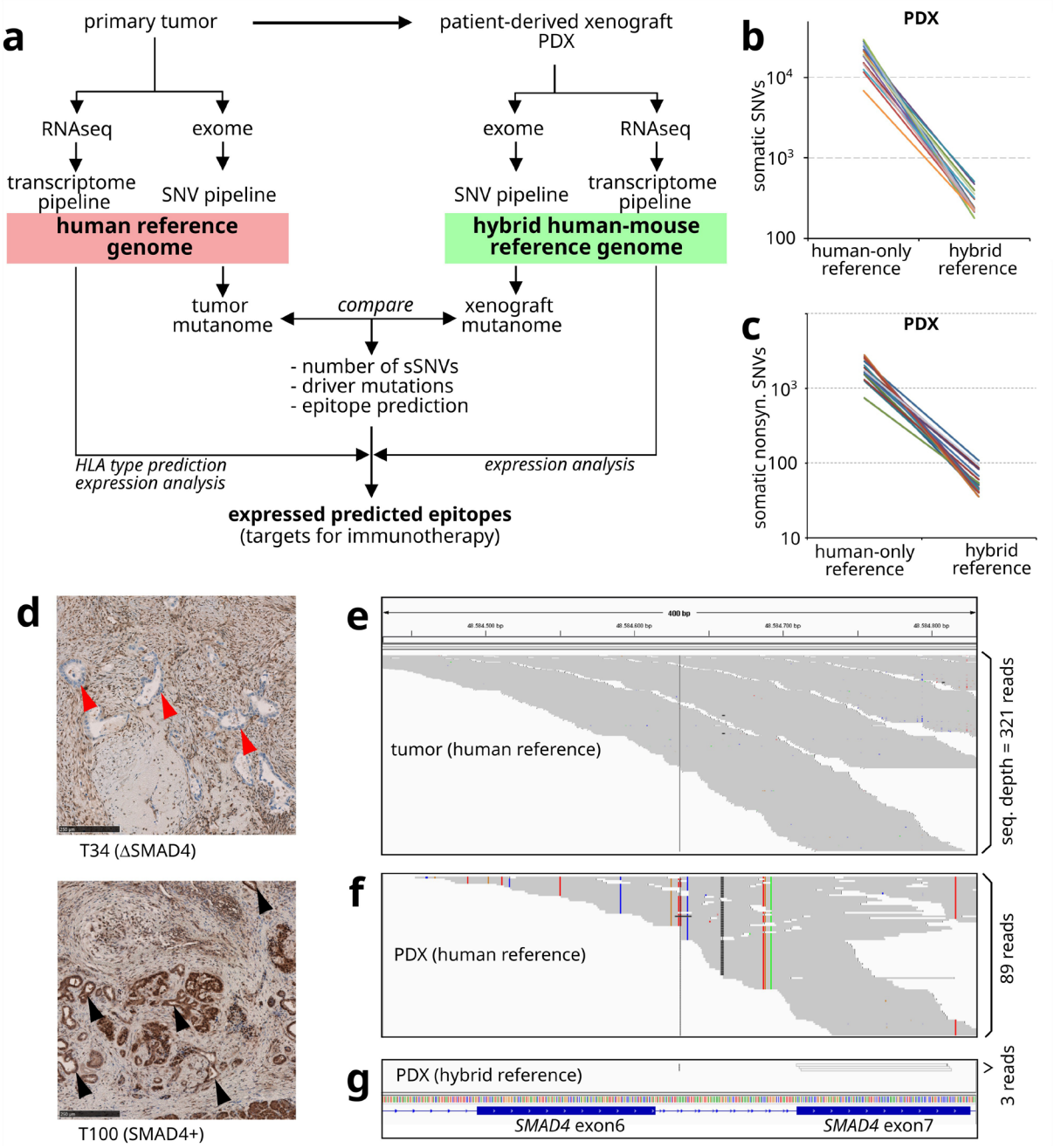

Figure 1 Summary of the T-cell neoepitope identification pipeline. (a) Primary tumor exomes were analyzed using a human reference genome (GRCh37/hg19) while the PDX exomes were analyzed using a hybrid reference genome consisting of the human chromosomes (GRCh37/hg19) and mouse chromosomes (GRCm38), adapted to comprise the SNPs of the NOD/ShiLtJ mouse strain. Expression of mutated alleles was assessed from RNA-seq data using the same procedure. RNA data were also used to define the HLA type of each sample. (b, c) Exclusion of mouse reads from PDX exome data by the hybrid reference genome. (d) Immunohistochemistry of primary tumor samples for SMAD4, revealing absence of SMAD4 from the tumor cells of sample T34 (red arrowheads; the other, SMAD4-positive cells are part of the tumor stroma). Tumor T100 shows strong SMAD4 expression in the tumor cells (black arrow heads). See online supplemental figure S1a for further examples of SMAD4-positive and negative tumors. (e) Analysis of exome data of sample T34, as exemplified in the context of a highly conserved (96%) 400 bp region encompassing exons 6 and 7 of the SMAD4 tumor suppressor gene, which contains 17 inter-species SNPs (online supplemental figure S1b). Analysis of exome data of the primary tumor sample with the human reference genome resulted in the mapping of 321 reads without mismatches. (f) Analysis of PDX exome data with the human reference genome resulted in the mapping of 89 reads, the majority of which showed one or more mismatches due to inter-species SNPs, marked by colored, vertical lines. (g) Analysis of PDX exome data with the hybrid reference genome resulted in mapping of all but three of the aforementioned reads to the mouse genome, thereby revealing a homozygous deletion for sample T34 in this part of the *SMAD4* locus. The remaining three reads are still mapped to the human genome because these fall within a sequence stretch that shares 100% homology between mouse and human (see online supplemental figure S1b). PDX, patient derived xenograft; RNA-seq, RNA sequencing; SNPs, single nucleotide polymorphisms; sSNVs, somatic single nucleotide variants, .

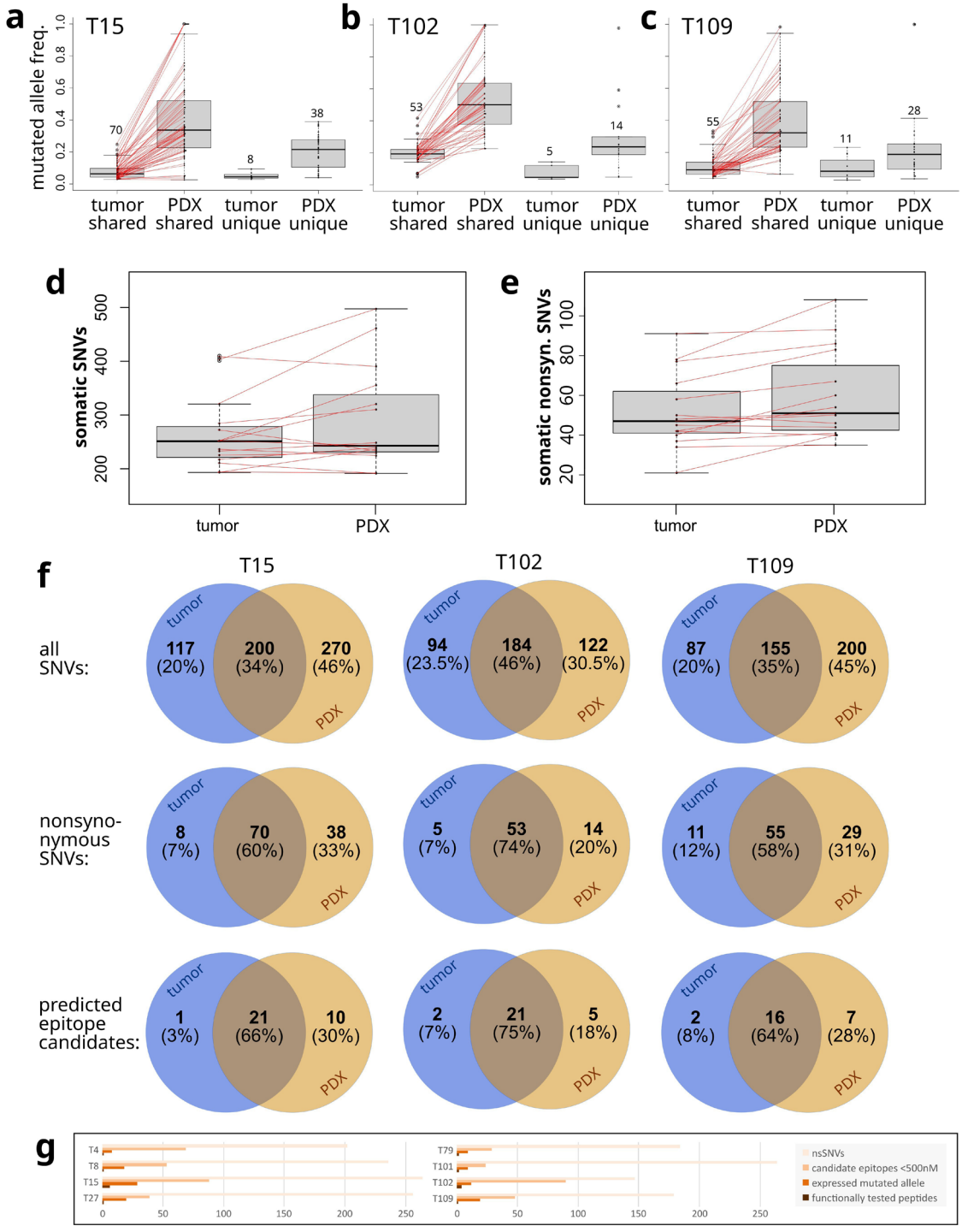

Figure 2 Increased sensitivity of mutation and T-cell epitope calling in PDX exomes. (a–c) Boxplots of the mutated allele frequency (MAF) of shared, tumor-unique somatic and PDX-unique somatic, non-synonymous SNVs for three selected datasets indicate that, for mutations detected in primary tumor as well as PDX, the MAF in the PDX is generally higher. See online supplemental figure S6 for all 15 data sets. (d) The number of somatic SNVs called from the exome data is in most cases higher in the PDX than in the corresponding primary tumor. (e) This difference is more prominent when only non-synonymous SNVs are considered. (f). Comparison of numbers of SNVs, nsSNVs and potential T-cell epitopes detected in primary tumor and PDX exomes. Shown are the data for tumor samples T15, T02 and T109. See online supplemental figure S8 for an overview on all eight HLA-A*02:01 positive tumor samples. (g) Graphic summary of the outcome of the mutation calling and neoepitope prediction workflow for the eight HLA-A*02:01 positive tumor samples involving, subsequently, nsSNV calling based on exome data, candidate neoepitope prediction with the NetMHC4.0 algorithm, verification of expression of the genes encoding aforementioned peptide sequences at the messenger RNA level, and selection of a set of 18 candidate neoepitopes based on a combination of most favorable parameters (primarily high predicted major histocompatibility complex binding affinity and expression of mutated allele) as detailed in online supplemental table S7. nsSNV, non-synonymous SNV; PDX, patient derived xenograft; SNV, single nucleotide variant.

Table 1 Retrospective evaluation of the NGS data underlying the calling of single nucleotide variants encoding the 18 candidate neoepitopes selected for immunological analyses

#	Epitope ID	Tumor MAF DNA	Reads	Tumor MAF RNA	Reads	PDX MAF DNA	Reads	PDX MAF RNA	Reads
1	ALDH4A1_R247H	0.33	26/78	- *	–	0.71	29/41	0.62	8/13
2	ATAD2_R913C	0.19	4/21	0.32	61/191	0.42	19/45	0.58	53/93
3	DNM3_R369H	0.15	14/91	0.1	2/20	0.62	67/108	0.61	3/4
4	FAM160B1_V418I	0.045	13/289	0.03	2/58	0.33	36/110	0.36	23/64
5	**FARP1_V785I**	**0.062**	**22/357**	**0.05**	**1/21**	**0.20**	**36/180**	**0.24**	**4/17**
6	**FILIP1L_F109V_a**	**0.16**	**26/164**	**0**	**0/7**	**0.65**	**106/164**	**0.71**	**5/7**
7	FILIP1L_F109V_b	0.16	26/164	0	0/7	0.65	106/164	0.71	5/7
8	KRAS_G12V	0.19	11/57	-*	–	0.58	21/36	0.68	27/40
9	NOTCH2_P1947A	0.29	49/166	-*	–	1	72/72	1	41/41
10	PAPSS1_A71T	0.33	27/83	0.56	63/112	0.99	75/76	1	227/227
11	**RABL6_K164E**	**0.19**	**12/64**	**0.22**	**21/96**	**0.73**	**66/91**	**0.72**	**78/108**
12	SLCO2A1_F338L_a	0	0/97	0	0/23	0.27	12/44	0.22	16/72
13	SLCO2A1_F338L_b	0	0/97	0	0/23	0.27	12/44	0.22	16/72
14	TP53_N131Y_a	0.27	20/74	0.33	4/12	1	42/42	1	2/2
15	TP53_N131Y_b	0.27	20/74	0.33	4/12	1	42/42	1	2/2
16	TRAM1_L256V	0.054	9/166	0.12	256/2129	0.15	21/136	0.17	173/1040
17	TRRAP_D859N	0.092	23/251	0.38	3/8	0.50	71/142	0.44	4/9
18	**TTC39A_S54R**	**0.034**	**10/292**	**0.29**	**9/29**	**0.21**	**32/153**	**0.20**	**20/98**

Summary of the output of the mutation calling pipeline as shown in figure 1a involving parallel analysis of NGS data from matched pairs of primary tumor and PDX samples. The data for the four neoepitopes against which T-cell receptors were generated is highlighted. Listed are the mutated allele frequencies and underlying read counts as determined based on whole exome and RNA sequencing. The read counts represent mutant/wild type sequence.
*In the case of candidate epitopes 1, 8 and 9, as identified in tumor samples T27 and T79, respectively (see online supplemental table S8), RNA quality as isolated from the primary tumor was insufficient to support RNA-sequencing.
MAF, mutated allele frequency; NGS, next generation sequencing; PDX, patient derived xenograft.

an MAF insufficient for statistical significance (online supplemental table S5). Although we cannot formally exclude the inclusion in our data sets of mutations that newly emerged in the PDX models, it is important to note that NGS was performed on the primary xenografts. Furthermore, none of the tumor samples included in this study carried mutations that would have resulted in chromosomal instability, for example, in DNA repair genes (online supplemental table S1), while newly emerged mutations are expected to have a low MAF. Data analysis also revealed small numbers of mutations uniquely found in primary tumor samples (figure 2a–c, online supplemental figure S6), probably reflecting tumor heterogeneity,[33] in particular tumor subclones under-represented in the PDX model. We deem it unlikely that either of these SNVs would represent sequencing/mutation calling artifacts, as we successfully verified the presence and MAF of several mutations by pyrosequencing (online supplemental figure S7 and table S6).

In summary, analysis of matched pairs of primary tumor samples and PDX models by means of the workflow shown in figure 1a markedly increases the sensitivity and accuracy of NGS-based mutation calling in PDAC. Notably, with the exception of recurrent mutations in KRAS, all mutations identified were unique for the individual tumors.

In silico and in vitro selection of candidate T-cell neoepitopes

While nsSNVs may encode T-cell neoepitopes, only a small fraction of the somatic mutations identified in tumors is expected to encode naturally processed, HLA-restricted, immunogenic peptide antigens.[20–26 34] We aimed at achieving proof of concept that several of the nsSNVs identified in our tumor panel encode neoepitopes that mediate T-cell recognition of tumor cells. We focused on HLA-A*02:01-restricted epitopes in view of the relative accuracy of the peptide binding algorithm, as well as the tools available for the experimental analysis of T-cell responses. Of the 15 PDAC samples included in our study, 8 were HLA-A*02:01-positive (online supplemental table S1). First, candidate epitopes encoded by the identified nsSNVs were screened in silico for potential HLA-A*02:01-binding using the NetMHC4.0 algorithm.[35] The numbers of candidate epitopes identified for each of the tumors based on exome data from primary tumor and/or PDX model are exemplified for three tumors in figure 2f (see online supplemental figure S8 for all tumors). These

data further demonstrate that for most of the samples, mutation calling and thereby mutanome-based epitope prediction is enhanced by our pipeline. Subsequently, we zoomed in on peptides encoded by mutant alleles expressed at the messenger RNA (mRNA) level using three expression datasets: RNA-seq of primary tumor, RNA-seq of the PDX model and publicly available PDAC transcriptome data.[36 37] Like the PDX DNA-seq data, the PDX RNA-seq data were analyzed with the hybrid reference genome to distinguish between the reads from human and mouse origin (figure 1a), resulting in data sets exclusively comprising reads from the human tumor cells. This enables a more accurate assessment of the relative expression of mutated versus wild type alleles, and is also likely to increase the sensitivity of mutated read detection, as compared with similar analysis of primary tumor transcriptome data. By means of this systematic approach, we found between 4 and 29 potential HLA-A*02:01-restricted neoepitopes to be expressed in each of the eight datasets (figure 2g, online supplemental table S7).

For our immunological studies, we focused on 18 candidate neoepitopes that showed a combination of good HLA affinity as predicted by the NetMHC algorithm and clearly detectable expression of the mutated allele in the PDX sample (figure 2g; see online supplemental tables S7 and S8 for details). Retrospective analysis of the mutanome data underlying the identification of the nsSNVs encoding these epitopes, in particular comparison of the mutated allele frequencies and read numbers from matching primary tumor and PDX samples, illustrates that our workflow resulted in a greatly increased confidence of mutation calling with respect to the corresponding nsSNVs at both the DNA and the RNA level (table 1). Actual HLA-A*02:01 binding of all peptides was confirmed by means of a commonly used cell-based assay that measures the stabilization of surface HLA expression in the presence of HLA-binding peptides[38] (figure 3a). A more stringent variant of this assay, in which the stabilization of surface HLA expression is measured at 37°C instead of 25°C, revealed that five of the mutant peptides show stronger HLA-binding than the wild-type counterparts (figure 3b, numbers 2, 4, 6, 8 and 12, marked with asterisks). This is primarily due to the greater half-life of the HLA/peptide complexes as determined in the time-course experiment (online supplemental figure S9), which is an important determinant of epitope immunogenicity.[39] Four additional peptides showed very strong and stable binding, independent of mutation (figure 3b and online supplemental figure S9, numbers 11, 13, 16 and 17, marked with pound sign).

Isolation of fully human, neoepitope-specific TCRs from peptide-immunized humanized mice

In-depth analysis of the selected candidate neoepitopes was performed by raising T-cell responses in transgenic mice that harbor the human TCR gene loci instead of the endogenous counterparts, and express HLA-A*02:01 instead of the murine major histocompatibility complex homologs.[30 40] The utilization of these mice enables the generation of fully human antigen-specific TCRs that could be used for TCR gene therapy in patients. In order to avoid the induction of T-cell immunity against antigenic determinants related to inter-species differences, the aforementioned selection of candidates for this study also included the criterion that the wild-type peptide sequence was conserved between human and mouse. As illustrated schematically in figure 4a, at least three HLA-A*02:01/huTCR-transgenic mice were immunized with each of the synthetic peptides representing the candidate neoepitopes. Blood cells from these mice were restimulated in vitro with the relevant peptides and subjected to immunofluorescence staining for interferon gamma (IFN-γ). In case significant numbers of peptide-reactive T cells were detected, splenocytes from reactive mice were FACS-sorted, after which the rearranged TCR-α and TCR-β genes were cloned by unbiased rapid amplification of complementary DNA ends-PCR from RNA of the sorted cells. The Vα and Vβ regions identified were inserted upstream of gene sequences encoding the murine orthologues of, respectively, the Cα and Cβ regions to avoid mispairing with endogenous TCR chains and facilitate detection of the transgene-encoded TCRs by means of flow cytometry.[40] For 10 candidate neoepitopes, peptide-reactive CD8+T cells could be detected in antigen-stimulated splenocyte cultures from immunized mice by means of flow cytometry and FACS-sorted to isolate mRNA. In the case of four neoepitopes, this resulted in the molecular cloning of one or more TCRs that conferred antigen-specific reactivity on expression in human T cells (online supplemental table S8). As mentioned above, the confidence of identifying these sequences as potential neoepitopes was markedly enhanced by our pipeline involving parallel analysis of NGS data from matching pairs of primary tumor and PDX samples (table 1). The very low mutated RNA read counts for mutations FARP1_V785I (1/21) and FILIP1L_F109V (0/7) in the primary tumor RNA-seq data would not have encouraged selection of the corresponding neoepitopes for the immunization experiments. The same applies to the low mutated allele frequencies for mutations FARP1_V785I (0.062) and TTC39A_S54R (0.034) in the primary tumor whole exome sequencing (WES) data.

Preliminary analysis of the TCRs raised against the candidate neoepitope peptides showed that these mediated T-cell responses with nanomolar sensitivity (figure 4b–e; online supplemental figure S10–S12). Furthermore, the TCRs displayed preferential reactivity against the mutated peptides as compared with their wild-type counterparts, although to different degrees. Three of the TCRs were raised against neoepitopes identified in tumor T15: TCR_FARP1, TCR_TTC39A#1 and TCR_TTC39A#2. The other two TCRs were raised against neoepitopes identified in, respectively, tumor T102 (TCR_FILIP1L) and tumor T109 (TCR_RABL6).

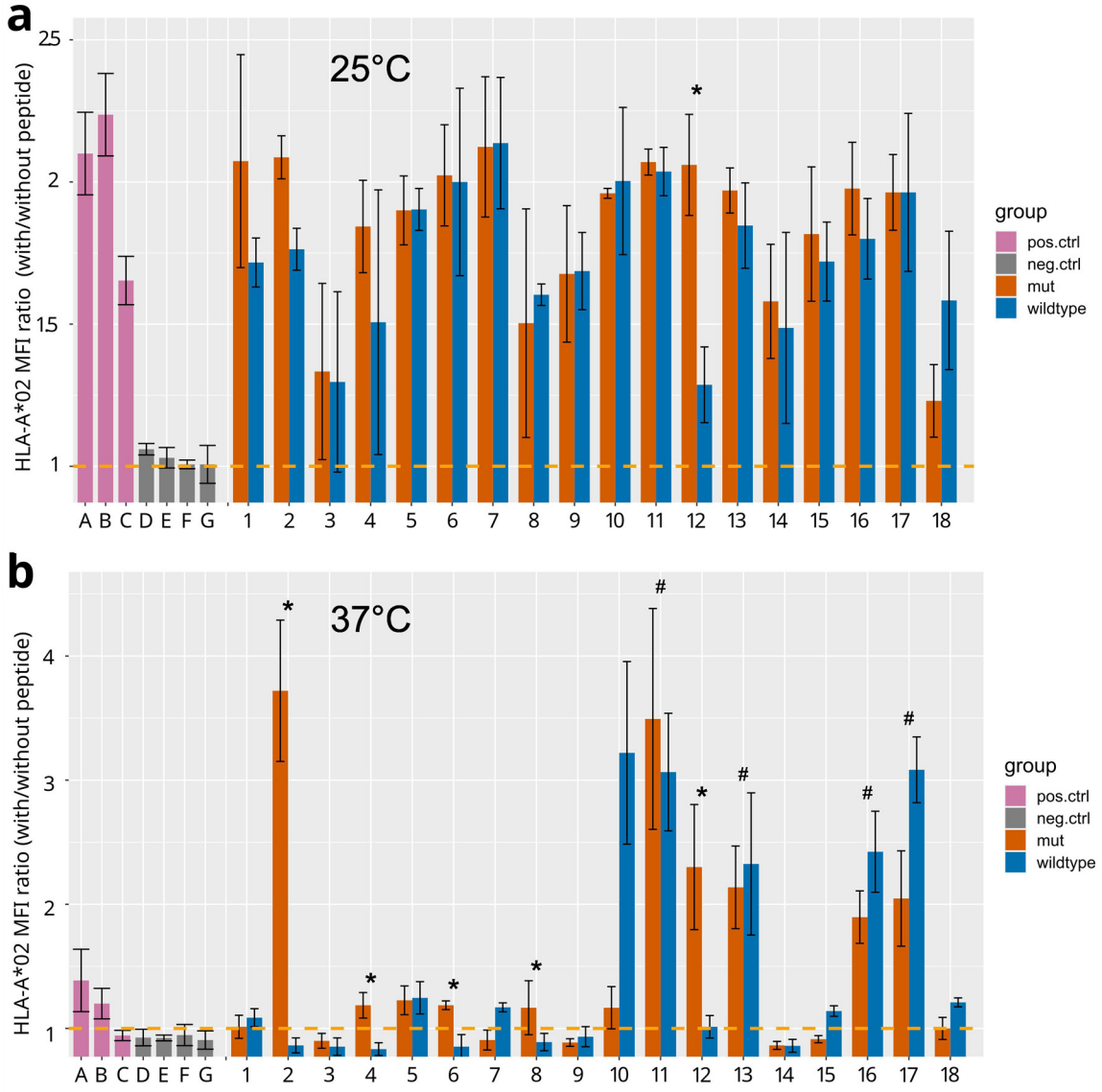

Figure 3 Experimental analysis of HLA-binding of predicted neoepitopes. HLA-A*02:01 binding of peptides representing the potential T-cell neoepitopes (orange) and their wild-type counterparts (blue) was assessed at 25°C (a) to confirm overall binding and 37°C (b) to distinguish strong from weaker binders. Numbers refer to the peptides listed in online supplemental table S8, which also lists the well-defined HLA-A*02:01 restricted epitopes that were used as positive (A–C) and negative (D–G) controls. Plotted are the ratios of FACS-derived HLA-A*02:01 MFI values of peptide-loaded T2 cells versus untreated T2 cells. Asterisks indicate significantly increased binding of the mutant peptide compared with the wildtype version; the pound sign highlights candidates with an overall high affinity to HLA-A*02:01 irrespective of the mutation. FACS, fluorescent activated cell sorting; MFI, mean fluorescent intensity.

Neoepitope-specific TCRs react against tumor cells expressing the mutated epitope-encoding genes

For functional TCR testing, methodologies were employed that we used successfully in a previously described study to screen the antitumor reactivity of multiple TCRs isolated from the TIL repertoire of nine human PDAC tumor samples.[15 41] This involved transient transfection of a human T-cell line (T222, see Materials and methods) largely consisting of CD8+T cells with in vitro transcribed mRNA encoding the TCR-α/β pairs of interest. All five TCRs expressed efficiently and reproducibly as verified by flow cytometry (online supplemental figure S13). The TCRs did not only mediate T-cell reactivity against exogenously loaded peptide antigen, but also against endogenously expressed antigen, in that they recognized antigen-presenting cells transduced with a multi-epitope gene construct encoding a string-of-beads arrangement of 30-mer peptide sequences that comprise the mutant neoepitopes in their natural context (figure 5a–e, left and middle panels, (online supplemental figure S14a,b). The availability of tumor lines derived from two of the human PDA tumors included in this study, T15 and T102, permitted analysis of antitumor reactivity for four of these TCRs. Importantly, all three TCRs raised against epitopes identified in the T15

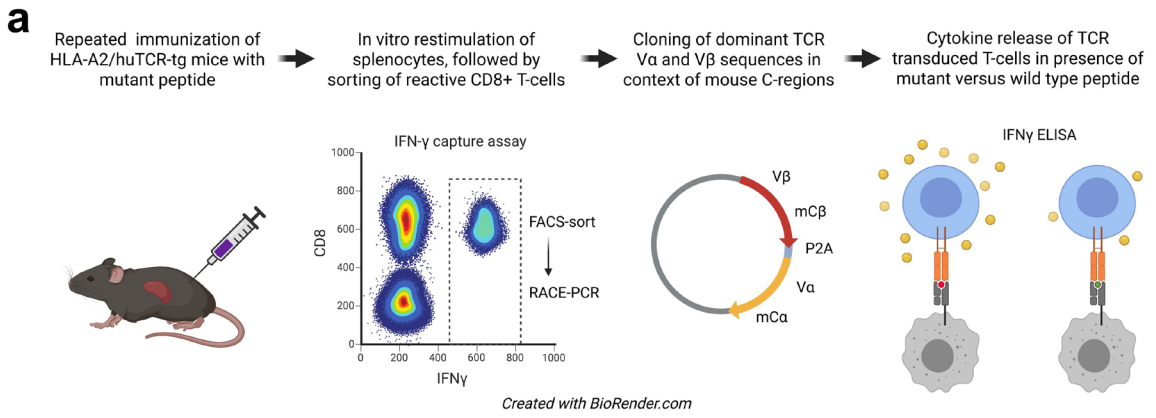

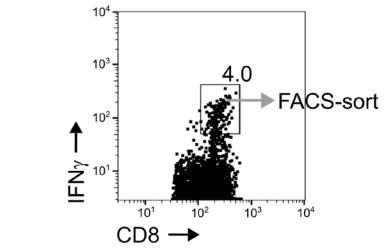

c TCR sequences reproducibly identified

TCR	V	J	CDR3 sequence	fraction
α1	TRAV26-1	TRAJ43	CIVRANNDMRF	7/14
α2	TRAV39	TRAJ48	CAVDISNFGNEKLTF	7/14
β1	TRBV27	TRBJ2-6	CASSLIFGANVLTF	7/13
β2	TRBV25-1	TRBJ2-3	CASSGRDTQYF	6/13

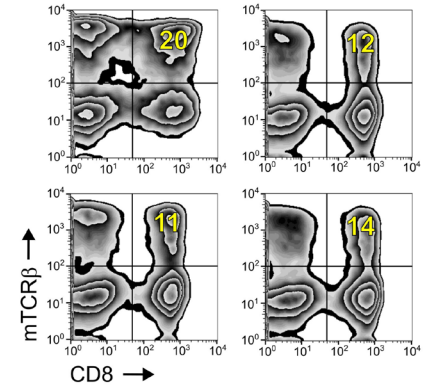

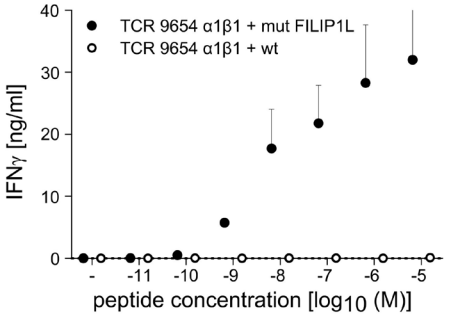

TCR 9654 α2β1, α1β2, α2β2: no peptide recognition

Figure 4 Generation of neoepitope-specific TCRs in HLA-A*02:01/human TCR locus transgenic mice. (a) Schematic overview of the workflow. Splenocytes from HLA-A*02:01 × human TCR-locus transgenic mice, repeatedly immunized with the synthetic peptide of interest, were cultured in the presence of the peptide concerned. Peptide-reactive CD8+T cells as identified by IFN-γ capture assay were sorted, after which the repertoire of TCR Vα and Vβ sequences was analyzed by 5'-RACE RT-PCR on the basis of RNA from these T cells. The most prominent Vα and Vβ sequences were cloned into retroviral expression vectors, upstream of the murine Cα and Cβ regions to allow for selective pairing and detection of cell-surface expression of the transgene encoded TCRs in primary human T cells. In case of identification of multiple Vα and/or Vβ sequences, all possible combinations were tested. The reactivity of efficiently expressed Vα/Vβ combinations against mutant and wild-type peptide epitopes was subsequently tested by means of IFN-γ ELISA. (b–e) Shown as an example is the isolation of the TCR against the 9-mer neoepitope FILIP1L_F109V as identified in tumor T102. See online supplemental figure S10–S12 for corresponding data for the other three primary neoepitopes. (b) Peptide-reactive T-cell population as detected in splenocyte culture of a mouse (ID #9654) repeatedly immunized with the FILIP1L_F109V peptide by means of IFN-γ capture assay in the presence of the relevant peptide. Shown are the cells in the CD3-positive gate. (c) TCR Vα and Vβ sequences identified by means of 5'-RACE RT-PCR in FACS-sorted T-cells. (d) Expression of the four different combinations of TCR alpha and beta chains identified on retroviral gene transduction into primary human PBMC. In this case, all four Valpha/Vbeta combinations were expressed and therefore tested for reactivity (d) Response of human T cells transduced with one of the four TCRα/β combinations (T9654a) against T2-cells loaded with titered concentrations of the FILIP1L_F109V 9-mer neoepitope of its wild-type counterpart. Neither of the other three TCR-α/β combinations mediated significant peptide epitope recognition to TCR-transduced T cells. FACS, fluoresence activated cell sorting; IFN, interferon; PBMC, peripheral blood mononuclear cells; RACE, rapid amplification of complementary DNA ends; TCR, T-cell receptor.

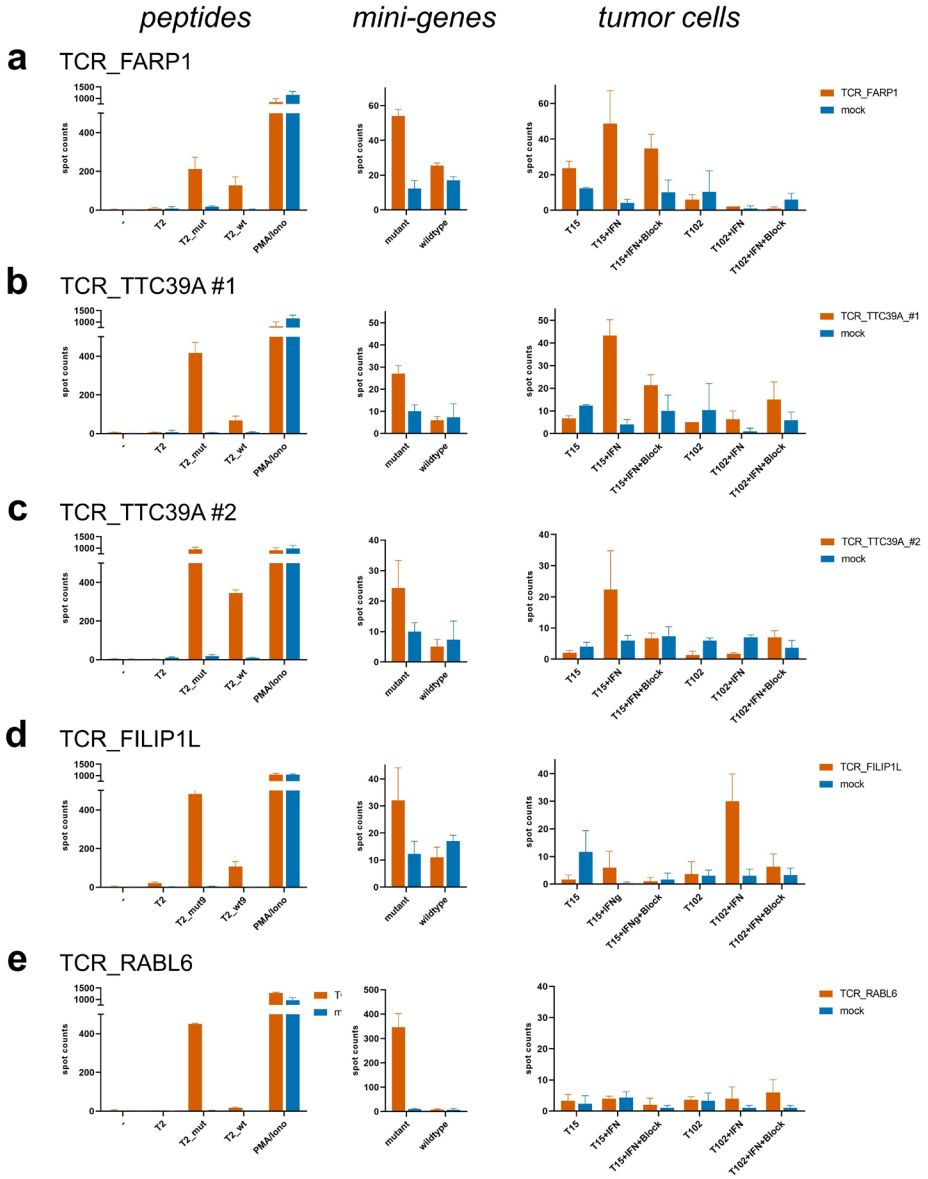

Figure 5 TCR-mediated T-cell reactivity against cognate peptide antigen and autologous pancreatic ductal adenocarcinoma tumor cells. Human T cells (T222 cell line, see Materials and methods) were transiently transfected with in vitro transcribed messenger RNA encoding the indicated TCR-α/β pairs, and subsequently incubated with the following antigen presenting cells: peptide-loaded T2 cells (left panels), autologous HLA-A*02:01+antigen presenting cells transduced with multi-epitope gene constructs encoding a string-of-beads arrangement of either the mutant or the wild-type peptide sequences of interest (middle panels), or T15 and T102 tumor cells (right panels). T-cell responses were measured by means of IFN-γ ELISpot assays as further detailed below. Spot counts represent the numbers of T cells that secreted IFN-γ as captured by anti-IFN-γ antibodies adhered at the bottom of the 96-well plates (see Materials and methods). (a, b, c) TCRs raised against the FARP1_V785I, and TTC39A_S54R neoepitopes identified in the T15 tumor sample. (d) TCR raised against the FILIP1L_F109V 9-mer neoepitope identified in the T102 tumor sample. (e) TCR raised against the RABL6_K164E neoepitope identified in the T109 sample. The T2 cells were pre-pulsed with synthetic peptides at a concentration of 5 µg/mL. Each TCR was tested against their cognate neoepitope peptide (T2_mut) and the wild-type counterpart (T2_wt). In the case of the multi-epitope gene constructs, the epitopes of interest, flanked on each side by 10 amino acids of natural sequence context, were incorporated into a string of beads arrangement that was inserted between the luminal and transmembrane of the LAMP1 protein to allow for efficient processing into major histocompatibility complex. The HLA-A*02:01 MART-1 epitope was added at the C-terminal end of the multi-epitope arrangement to serve as internal positive control through its recognition by DMF5 TCR-transduced T cells (online supplemental figure S14). In these experiments, multi-epitope gene constructs were transfected into T222 cells, which express HLA-A*02:01, to create a fully autologous T-cell/antigen presenting cell setting. Antitumor reactivity was measured against IFN-γ-pretreated (T15+IFN; T102+IFN) and non-treated (T15; T102) tumor cells, as well as in the presence of pan-HLA class I antibody W6/32 (block). Mock-transduced T-cells and stimulation with PMA/ionomycin served as negative and positive controls, respectively. Responses were measured after 24 hours co-cultivation by means of IFN-γ ELISpot. Each TCR was tested in at least two independent experiments with similar outcome. ELIspot, enzyme-linked immunosorbent spot; IFN, interferon; PMA, phorbol-12-myristate-13acetate; TCR, T-cell receptor.

tumor sample mediated T-cell activation in the presence of autologous T15 tumor cells, but not against T102 tumor cells. This recognition was enhanced when the tumor cells were pretreated with IFN-γ (figure 5a–c, right panels), in line with the increased cell surface expression of the HLA-A*02:01 molecule (online supplemental figure 14C), and the IFN-γ-induced enhancement of antigen processing into HLA class I.[42] Furthermore, T-cell reactivity was reduced in the presence of the pan-HLA antibody W6/32 (figure 5a–c). The fourth TCR, raised against the FILIP1L_F109V epitope as identified in tumor T102, showed a reciprocal reactivity pattern, in that it mediated T-cell reactivity against T102 cells, but not T15 cells. Again, antitumor reactivity was enhanced by IFN-γ pretreatment of the tumor cells, and suppressed by W6/32 (figure 5d). The fifth TCR was raised against the RABL6_K164E neoepitope as identified in tumor T109. Although the lack of an autologous cell line for this tumor precluded testing of this TCR for tumor reactivity, it provided a further experimental control, in that T cells expressing this TCR did not respond to either T15 or T102 cells (figure 5e). In order to consolidate the physiological relevance of the TCR targeting the RABL6_K164E neoepitope, we transfected antigen-presenting cells with full-length gene constructs of the mutated and wild-type RABL6 gene. As shown in figure 6a, only expression of the mutated gene construct resulted in TCR-mediated T-cell activation.

Taken together, these data show that TCR reactivity is highly selective against cells expressing the mutated genes of interest, in spite of the fact that two of these TCRs (TCR_FARP1 and TCR_TC39A_#2; see figure 5, left panels) show prominent reactivity against exogenously loaded wild-type peptides. However, in these experiments supraphysiological peptide concentrations (5 µM) were used for target cell loading. Pulsing of the antigen-presenting cells with titered amounts of synthetic peptides revealed that even for these two TCRs there is at least a 1-log difference between immunogenic concentrations of the mutant and wild-type peptide, with exclusive T-cell reactivity against the mutant peptide observed at synthetic peptide concentrations in the 10–100 picomolar range (figure 6b). The different levels of TCR reactivity to the wild-type peptides duly reflect the impact of the amino acid substitutions on the HLA/peptide complex. The phenylalanine to valine substitution in the FILIP1L sequence affects the C-terminal anchor residue, valine being the preferred residue at this position,[35] therefore likely to mediate enhanced HLA-binding of the mutated peptide (figure 3b). In the other three neoepitopes, the key anchor residues (position two and the C-terminal residue) are not affected by the mutations. In the RABL6 epitope, substitution of the positively charged lysine to a negatively charged glutamic acid is expected to prominently affect TCR engagement (figure 6c). Modeling of the HLA/peptide complex furthermore shows that the serine to arginine substitution of the N-terminal residue in the TTC39A epitope also creates a distinct interface with the TCR, however, in a decentralized location. This may explain the different degree of reactivity of the two TCRs to the wild-type peptide (figure 6b) due to a different relative orientation of these TCRs to the HLA/peptide complex.[43] The higher degree of reactivity by the FARP1-specific TCR to the wild-type sequence is in line with the subtle valine to isoleucine substitution in the corresponding epitope (figure 6b,c).

DISCUSSION

In this study, we provide proof of concept for the induction of HLA-restricted, tumor-reactive T-cell responses targeting mutanome-encoded neoepitopes as identified in human PDAC tumors. Mutation calling based on DNA and RNA preparations of primary tumor samples from PDAC and other cancer types with high stromal content is hampered by the fact that the mutated sequencing reads from the tumor cells are diluted by wild type reads from stromal cells. Consequently, mutations are detected with low confidence, or even missed. We therefore developed a pipeline for enhanced mutanome analysis, involving parallel analysis of matched primary tumor and PDX samples. Although PDX samples also comprise stromal cells, these are of mouse origin. The application of a customized hybrid reference genome provided unambiguous distinction between the human and mouse reads in the PDX samples, thereby markedly increasing the sensitivity of SNV calling. This allowed accurate determination of the mutated allele frequency as well as mRNA expression level of the mutated allele. By applying these criteria, in combination with in silico prediction of HLA-binding affinity and confirmation of actual HLA-binding in cell-based assays, we selected 18 candidate neoepitopes for immunological validation. For four of these, immunization of humanized mice resulted in the isolation of fully human TCRs by molecular cloning. The finding that these TCRs specifically recognize naturally processed antigen on the tumor cells in which the neoepitopes were identified, and/or cells transfected with the relevant HLA/antigen combination, demonstrates the feasibility of eliciting tumor-reactive T-cell responses through neoepitope immunization, even for poorly immunogenic pancreatic cancers. Notably, inclusion of the PDX model NGS data in the mutanome analysis proved essential for the selection of three of these neoepitopes, in that the detection of the corresponding DNA-mutations and/or mutant RNA-transcripts in the primary tumor NGS data was poor (table 1).

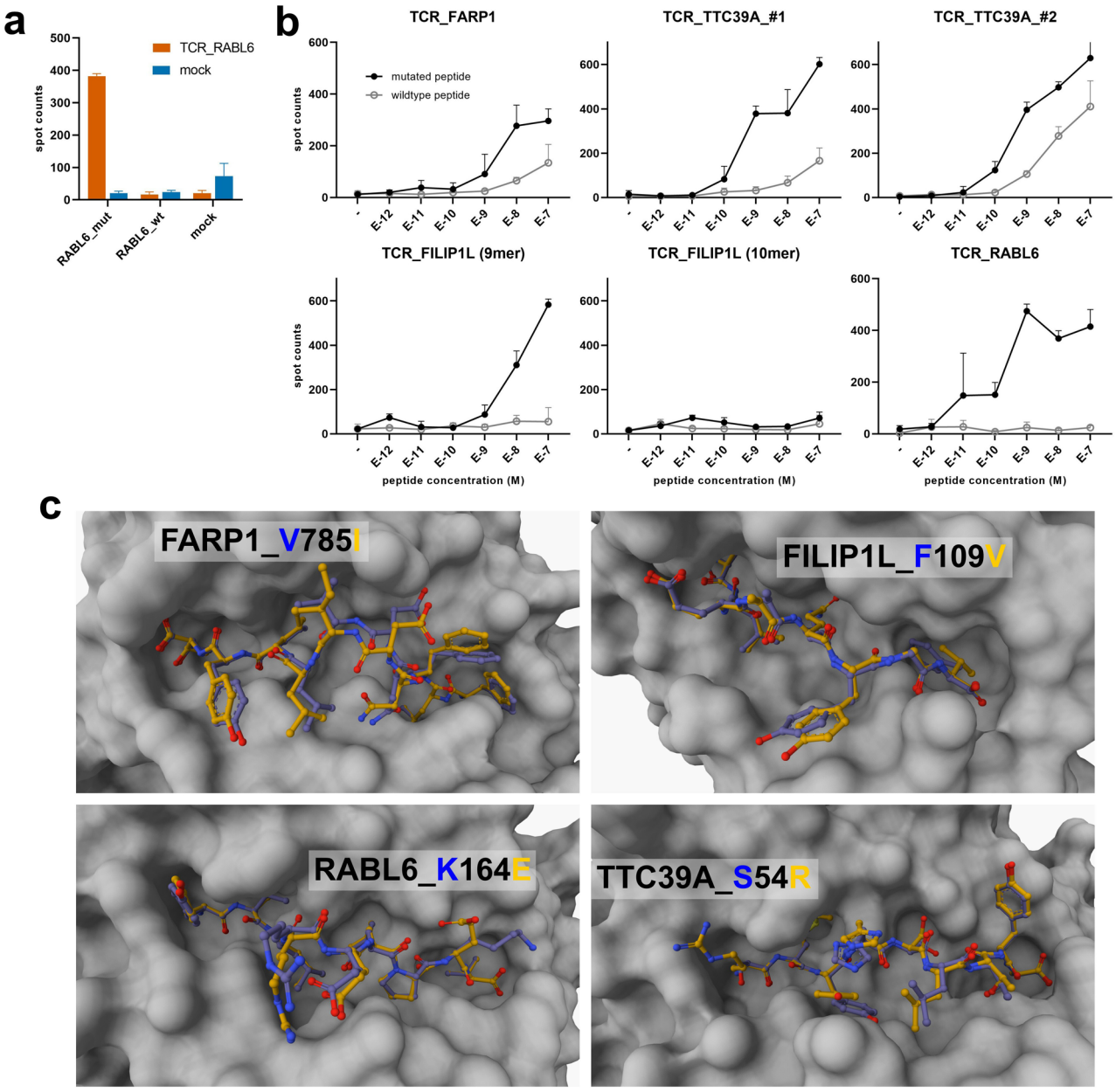

Figure 6 TCR-mediated T-cell reactivity against naturally processed antigen and limiting antigen concentrations. Human T cells were transduced with the indicated TCRs as in figure 5 and incubated with (a) HLA-A*02:01+antigen presenting cells transiently RNA-transfected with full-length gene constructs encoding the K164E-mutated or wild-type RABL6 antigen (b) T-2 cells loaded with indicated concentrations of the cognate peptide epitope or its wild-type counterpart. Responses by T cells transduced with the indicated TCR were measured after 24 hours co-cultivation by means of IFN-γ ELISpot. Each TCR was tested in two independent experiments with similar outcome. Data obtained show good correspondence with initial TCR screenings as depicted in figure 4e and online supplemental figures S10–12. (c) Models for binding of the indicated wild-type (purple) and mutant (ochre) peptides to the peptide binding groove of HLA-A*02:01, as generated using PANDORA (version 2.0.0b2) with n_loop_models=1000 and loop_refinement=slow. The best model was defined using molpdf score and visualized using Mol* Viewer (https://molstar.org/viewer/). The primary sequences of the neoepitopes shown are as follows (substituted amino acid underlined). FARP1_V785I: FLFND<u>I</u>LLYT, FILIP1L_F109V: ALLEAQYG<u>V</u>, RABL6_K164E: YILRELP<u>E</u>V, TTC39A_S54R: RMYHSLTYA. ELIspot, enzyme-linked immunosorbent spot; IFN, interferon; TCR, T-cell receptor.

A limitation of our proof of concept experiments is that the selection and immunological validation of neoepitopes was focused on HLA-A*02:01. Since a majority of published T-cell epitope studies have focused on this HLA molecule, due to its high prevalence in the Caucasian population, the prediction for HLA binding is expected to be more accurate than for less prevalent—and therefore less studied—HLA molecules. Nevertheless, mutation calling with improved sensitivity and confidence at the level of both exome and transcriptome, the main innovative aspect of our pipeline, will also facilitate the identification

of candidate neoepitopes restricted by other HLA molecules. A further limitation of our study is that the epitopes and corresponding TCRs as described in our study concern patient-unique, "private" epitopes and therefore could only be applied in individualized immunotherapy. Notably, this is an issue intrinsic to PDAC, in that all mutations detected in our tumor samples, except for those in the K-ras oncogene, were non-recurrent. In spite of multiple attempts, we were not able to raise specific T-cell responses against the $KRAS^{G12V}$-derived HLA-A*02:01-binding neoepitope KLVVVGAVGV. Accordingly, others have shown that this peptide does not represent a naturally presented epitope in the context of HLA-A*02:01.[44 45] In a separate study, immunization of HLA-A*02:01/human TCR-transgenic mice with proteasome-spliced versions of this peptide (spliceotopes; KLVV/GAVGV and KLVVV/AVGV)[46] did result in the isolation of high-affinity, neoepitope specific TCRs. However, these TCRs failed to react against $KRAS^{G12V}$/HLA-A*02:01-expressing tumor cells due to the lack of naturally processed antigen.[47] This illustrates that candidate neoepitopes not reflecting naturally processed antigens can readily elicit therapeutically irrelevant T-cell responses. Earlier studies have similarly shown that only a small fraction of the candidate T-cell epitopes, as predicted by means of algorithms, HLA-binding assays and immunization experiments using synthetic peptides, represent physiologically relevant T-cell epitopes.[21 23 25 26 34]

Due to the restrictions shaping the natural immunopeptidome, also the number of true T-cell epitopes derived from oncogenic driver mutations, such as in RAS oncogenes and p53, is limited to select combinations of mutations and HLA-molecules.[27 44 48–51] Therefore, even the therapeutic application of TCRs targeting recurrent mutations in oncoproteins is restricted to a select patient subset,[26 45] whereas TCRs targeting tumor-associated autoantigens have the risk of inflicting dose-limiting toxicity in normal somatic tissues.[52–54] Hence, it is important to further invest in the exploration of neoepitopes for personalized immunization and TCR gene therapy, especially for the treatment indications such as PDAC that are not responsive to immune checkpoint inhibitor regimens due to the limited magnitude of the endogenous T-cell response.

Author affiliations
[1]Department of General, Visceral and Transplantation Surgery, University Hospital Heidelberg, Heidelberg, Germany
[2]Division of Molecular Oncology of Gastrointestinal Tumors, German Cancer Research Center, Heidelberg, Germany
[3]Institute of Tumor Immunology, Charité - Universitätsmedizin Berlin, Berlin, Germany
[4]Division of Experimental and Translational Tumor Immunology, German Cancer Research Center, Heidelberg, Germany
[5]Division of Omics IT and Data Management, German Cancer Research Center, Heidelberg, Germany
[6]Division of Immunotherapy and Immunoprevention, German Cancer Research Center, Heidelberg, Germany
[7]Division of Stem Cells and Cancer and HI-Stem, German Cancer Research Center, Heidelberg, Germany
[8]Max Delbruck Centre for Molecular Medicine in the Helmholtz Association, Berlin, Germany

Present affiliations The present affiliation of Michael Volkmar is: Cellular Therapies Platform, Helmholtz Institute for Translational Oncology (HI-TRON) Mainz, Mainz, Germany and Dana Hoser is: T-knife, Therapeutics Inc, Berlin, Germany.

Acknowledgements We are grateful for the support by the DKFZ Genomics and Proteomics core facility with respect to next generation sequencing (Stephan Wolf and colleagues), and by the DKFZ Central Animal Facility (Kurt Reifenberg and colleagues) for the development of PDX models. For excellent help and support during sample collection, we thank the biobanks of (1) the European Pancreas Center (EPZ) at Heidelberg University Hospital, (2) the National Center for Tumor Diseases (NCT), Heidelberg, (3) the Department of Pathology at Heidelberg University Hospital, especially Dr Frank Bergmann and Dr Esther Herpel. Activities of the EPZ-Pancobank were supported by the Heidelberger Stiftung Chirurgie and in part by the German Ministry of Science and Education (BMBF) grants 01ZX1305C, 01ZX1605C, 01KT1506. The EPZ-Pancobank is chaired by Professor Dr M W Büchler, assisted by Dr N A Giese, Dr M Schenk, and M Fischer, and is a member of the BioMaterial Bank Heidelberg/BMBH (supervisor: Professor P Schirmacher, BMBF grant#01EY1701) belonging to the German Biobank Alliance. We thank Sabrina Horn and Kathrin Borgwald for excellent technical support. The authors would like to thank Mogjiborahman Salek, Jonas Förster, Christian Lehmann and Sven Blobner for additional experiments performed in the context of this study that were not included in the final manuscript.

Contributors RO (guarantor), MV and GW designed the study and wrote the manuscript. MV, CL, JRe and AH-W were involved in tumor mutanome analysis. CL, IP and JRi performed the experiments related to the immunogenicity of the candidate peptide epitopes and the functional analysis of the TCRs. The TCRs were isolated from immunized, HLA/human TCR-transgenic mice by DH under the supervision of GW and TB. The T15 and T102 tumor cell lines were provided by MS and AT. HLA/peptide complex modelling was performed by JPB and ABR. All clinical samples underlying this study were provided by the biobank of the European Pancreas Center under supervision of OS.

Funding The work as performed at the German Cancer Research Center was financially supported by the KH Bauer Foundation (to RO, MV, JR and IP), the Graduate School of the German Cancer Research Center (to JRi), as well as through the PANC-STRAT consortium through the Federal Ministry of Education and Research (BMBF 01ZX1605C; to CL, MS and AT) and the German Cancer Consortium (DKTK Grant NEO-ATT; to CL and GW). Part of the next generation sequencing effort was financed through the Heidelberg Center for Personalized Oncology (HIPO) through the National Center for Tumor Diseases (HIPO015, NCT: to MV and RO). This work was further supported by grants from the German Cancer Aid (111549, to GW, TB, RO), the European Union (ERC Advanced Grant 882963) (TB) the Berlin Institute of Health (BIH) through a collaborative research grant (T-cell gene therapy of cancer; TB) and the Helmholtz-Gemeinschaft, Zukunftsthema 'Immunology and Inflammation' (ZT-0027, to RO, TB). Activities of the EPZ-Pancobank were supported by the Heidelberger Stiftung Chirurgie and in part by the German Ministry of Science and Education (BMBF) grants 01EY1701, 01ZX1305C, 01ZX1605C, and 01KT1506. For the publication fee, we acknowledge financial support by Heidelberg University.

Competing interests None declared.

Patient consent for publication Not applicable.

Ethics approval The study was approved by the local ethics committees (Universität Heidelberg, Ethikkommision der Medizinische Fakultät; https://www.medizinische-fakultaet-hd.uni-heidelberg.de/fakultaet/kommissionen/ethikkommission; Ethikvotum Nr. S-708/2019; Title: Aufbau einer Blutzellen-, Serum- und Gewebebank für molekularbiologische Untersuchungen und zur Etablierung diagnostischer und prognostischer Marker benigner und maligner Erkrankungen des Gastrointestinaltraktes und der endokrinen Organe) and conducted in accordance with the declaration of Helsinki.

Provenance and peer review Not commissioned; externally peer reviewed.

Data availability statement All data relevant to the study are included in the article or uploaded as supplementary information.

ORCID iDs
Isabel Poschke http://orcid.org/0000-0002-4387-5566
Gerald Willimsky http://orcid.org/0000-0002-9693-948X
Rienk Offringa http://orcid.org/0000-0001-6310-1026

REFERENCES

1 Connor AA, Denroche RE, Jang GH, *et al*. Association of Distinct Mutational Signatures With Correlates of Increased Immune Activity in Pancreatic Ductal Adenocarcinoma. *JAMA Oncol* 2017;3:774–83.
2 Ho WJ, Jaffee EM, Zheng L. The tumour microenvironment in pancreatic cancer - clinical challenges and opportunities. *Nat Rev Clin Oncol* 2020;17:527–40.
3 Morrison AH, Byrne KT, Vonderheide RH. Immunotherapy and Prevention of Pancreatic Cancer. *Trends Cancer* 2018;4:418–28.
4 Ali LR, Lenehan PJ, Cardot-Ruffino V, *et al*. PD-1 Blockade Induces Reactivation of Nonproductive T-Cell Responses Characterized by NF-κB Signaling in Patients with Pancreatic Cancer. *Clin Cancer Res* 2024;30:542–53.
5 Ene-Obong A, Clear AJ, Watt J, *et al*. Activated pancreatic stellate cells sequester CD8+ T cells to reduce their infiltration of the juxtatumoral compartment of pancreatic ductal adenocarcinoma. *Gastroenterology* 2013;145:1121–32.
6 Fukunaga A, Miyamoto M, Cho Y, *et al*. CD8+ tumor-infiltrating lymphocytes together with CD4+ tumor-infiltrating lymphocytes and dendritic cells improve the prognosis of patients with pancreatic adenocarcinoma. *Pancreas* 2004;28:e26–31.
7 Gros A, Tran E, Parkhurst MR, *et al*. Recognition of human gastrointestinal cancer neoantigens by circulating PD-1+ lymphocytes. *J Clin Invest* 2019;129:4992–5004.
8 Łuksza M, Sethna ZM, Rojas LA, *et al*. Neoantigen quality predicts immunoediting in survivors of pancreatic cancer. *Nature New Biol* 2022;606:389–95.
9 Parkhurst MR, Robbins PF, Tran E, *et al*. Unique Neoantigens Arise from Somatic Mutations in Patients with Gastrointestinal Cancers. *Cancer Discov* 2019;9:1022–35.
10 Poschke I, Faryna M, Bergmann F, *et al*. Identification of a tumor-reactive T-cell repertoire in the immune infiltrate of patients with resectable pancreatic ductal adenocarcinoma. *Oncoimmunology* 2016;5:e1240859.
11 Poschke IC, Hassel JC, Rodriguez-Ehrenfried A, *et al*. The Outcome of *Ex Vivo* TIL Expansion Is Highly Influenced by Spatial Heterogeneity of the Tumor T-Cell Repertoire and Differences in Intrinsic *In Vitro* Growth Capacity between T-Cell Clones. *Clin Cancer Res* 2020;26:4289–301.
12 Stossel C, Raitses-Gurevich M, Atias D, *et al*. Spectrum of Response to Platinum and PARP Inhibitors in Germline *BRCA* –Associated Pancreatic Cancer in the Clinical and Preclinical Setting . *Cancer Discov* 2023;13:1826–43.
13 Stromnes IM, Hulbert A, Pierce RH, *et al*. T-cell Localization, Activation, and Clonal Expansion in Human Pancreatic Ductal Adenocarcinoma. *Cancer Immunol Res* 2017;5:978–91.
14 Yossef R, Tran E, Deniger DC, *et al*. Enhanced detection of neoantigen-reactive T cells targeting unique and shared oncogenes for personalized cancer immunotherapy. *JCI Insight* 2018;3:e122467.
15 Meng Z, Rodriguez Ehrenfried A, Tan CL, *et al*. Transcriptome-based identification of tumor-reactive and bystander $CD8^+$ T cell receptor clonotypes in human pancreatic cancer. *Sci Transl Med* 2023;15:eadh9562.
16 Zheng C, Fass JN, Shih Y-P, *et al*. Transcriptomic profiles of neoantigen-reactive T cells in human gastrointestinal cancers. *Cancer Cell* 2022;40:410–23.
17 Rojas LA, Sethna Z, Soares KC, *et al*. Personalized RNA neoantigen vaccines stimulate T cells in pancreatic cancer. *Nature New Biol* 2023;618:144–50.
18 Ott PA, Hu Z, Keskin DB, *et al*. An immunogenic personal neoantigen vaccine for patients with melanoma. *Nature New Biol* 2017;547:217–21.
19 Sahin U, Oehm P, Derhovanessian E, *et al*. An RNA vaccine drives immunity in checkpoint-inhibitor-treated melanoma. *Nature New Biol* 2020;585:107–12.
20 Bassani-Sternberg M, Coukos G. Mass spectrometry-based antigen discovery for cancer immunotherapy. *Curr Opin Immunol* 2016;41:9–17.
21 Blankenstein T, Leisegang M, Uckert W, *et al*. Targeting cancer-specific mutations by T cell receptor gene therapy. *Curr Opin Immunol* 2015;33:112–9.
22 Haen SP, Löffler MW, Rammensee H-G, *et al*. Towards new horizons: characterization, classification and implications of the tumour antigenic repertoire. *Nat Rev Clin Oncol* 2020;17:595–610.
23 Paul S, Grifoni A, Peters B, *et al*. Major Histocompatibility Complex Binding, Eluted Ligands, and Immunogenicity: Benchmark Testing and Predictions. *Front Immunol* 2019;10:3151.
24 Rock KL, Reits E, Neefjes J. Present Yourself! By MHC Class I and MHC Class II Molecules. *Trends Immunol* 2016;37:724–37.
25 Srivastava PK. Cancer neoepitopes viewed through negative selection and peripheral tolerance: a new path to cancer vaccines. *J Clin Invest* 2024;134:e176740.
26 Pearlman AH, Hwang MS, Konig MF, *et al*. Targeting public neoantigens for cancer immunotherapy. *Nat Cancer* 2021;2:487–97.
27 Leidner R, Sanjuan Silva N, Huang H, *et al*. Neoantigen T-Cell Receptor Gene Therapy in Pancreatic Cancer. *N Engl J Med* 2022;386:2112–9.
28 Biankin AV, Waddell N, Kassahn KS, *et al*. Pancreatic cancer genomes reveal aberrations in axon guidance pathway genes. *Nature New Biol* 2012;491:399–405.
29 Cancer Genome Atlas Research Network. Electronic address: andrew_aguirre@dfci.harvard.edu, Cancer Genome Atlas Research Network. Integrated Genomic Characterization of Pancreatic Ductal Adenocarcinoma. *Cancer Cell* 2017;32:185–203.
30 Li L-P, Lampert JC, Chen X, *et al*. Transgenic mice with a diverse human T cell antigen receptor repertoire. *Nat Med* 2010;16:1029–34.
31 Noll EM, Eisen C, Stenzinger A, *et al*. CYP3A5 mediates basal and acquired therapy resistance in different subtypes of pancreatic ductal adenocarcinoma. *Nat Med* 2016;22:278–87.
32 Keane TM, Goodstadt L, Danecek P, *et al*. Mouse genomic variation and its effect on phenotypes and gene regulation. *Nature New Biol* 2011;477:289–94.
33 Connor AA, Gallinger S. Pancreatic cancer evolution and heterogeneity: integrating omics and clinical data. *Nat Rev Cancer* 2022;22:131–42.
34 Lehmann AA, Zhang T, Reche PA, *et al*. Discordance Between the Predicted Versus the Actually Recognized CD8+ T Cell Epitopes of HCMV pp65 Antigen and Aleatory Epitope Dominance. *Front Immunol* 2020;11:618428.
35 Andreatta M, Nielsen M. Gapped sequence alignment using artificial neural networks: application to the MHC class I system. *Bioinformatics* 2016;32:511–7.
36 Zhang G, He P, Tan H, *et al*. Integration of metabolomics and transcriptomics revealed a fatty acid network exerting growth inhibitory effects in human pancreatic cancer. *Clin Cancer Res* 2013;19:4983–93.
37 Zhang G, Schetter A, He P, *et al*. DPEP1 Inhibits Tumor Cell Invasiveness, Enhances Chemosensitivity and Predicts Clinical Outcome in Pancreatic Ductal Adenocarcinoma. *PLoS ONE* 2012;7:e31507.
38 Nijman HW, Houbiers JG, Vierboom MP, *et al*. Identification of peptide sequences that potentially trigger HLA-A2.1-restricted cytotoxic T lymphocytes. *Eur J Immunol* 1993;23:1215–9.
39 van der Burg SH, Visseren MJ, Brandt RM, *et al*. Immunogenicity of peptides bound to MHC class I molecules depends on the MHC-peptide complex stability. *The Journal of Immunology* 1996;156:3308–14.
40 Obenaus M, Leitão C, Leisegang M, *et al*. Identification of human T-cell receptors with optimal affinity to cancer antigens using antigen-negative humanized mice. *Nat Biotechnol* 2015;33:402–7.
41 Rodriguez Ehrenfried A, Zens S, Steffens L, *et al*. T-Cell-Based Platform for Functional Screening of T-Cell Receptors Identified in Single-Cell RNA Sequencing Data Sets of Tumor-Infiltrating T Cells. *Bio Protoc* 2024;14.
42 Strehl B, Seifert U, Krüger E, *et al*. Interferon-gamma, the functional plasticity of the ubiquitin-proteasome system, and MHC class I antigen processing. *Immunol Rev* 2005;207:19–30.

43 Hennecke J, Wiley DC. T cell receptor-MHC interactions up close. *Cell* 2001;104:1–4.
44 Bear AS, Blanchard T, Cesare J, *et al*. Biochemical and functional characterization of mutant KRAS epitopes validates this oncoprotein for immunological targeting. *Nat Commun* 2021;12:4365.
45 Linette GP, Bear AS, Carreno BM. Facts and Hopes in Immunotherapy Strategies Targeting Antigens Derived from KRAS Mutations. *Clin Cancer Res* 2024;30:2017–24.
46 Mishto M, Mansurkhodzhaev A, Ying G, *et al*. An in silico—in vitro Pipeline Identifying an HLA-A*02:01+ KRAS G12V+ Spliced Epitope Candidate for a Broad Tumor-Immune Response in Cancer Patients. *Front Immunol* 2019;10:2572.
47 Willimsky G, Beier C, Immisch L, *et al*. In vitro proteasome processing of neo-splicetopes does not predict their presentation in vivo. *Elife* 2021;10:e62019.
48 Douglass J, Hsiue EH-C, Mog BJ, *et al*. Bispecific antibodies targeting mutant RAS neoantigens. *Sci Immunol* 2021;6.
49 Kim SP, Vale NR, Zacharakis N, *et al*. Adoptive Cellular Therapy with Autologous Tumor-Infiltrating Lymphocytes and T-cell Receptor–Engineered T Cells Targeting Common p53 Neoantigens in Human Solid Tumors. *Cancer Immunol Res* 2022;10:932–46.
50 Peri A, Greenstein E, Alon M, *et al*. Combined presentation and immunogenicity analysis reveals a recurrent RAS.Q61K neoantigen in melanoma. *J Clin Invest* 2021;131:e129466.
51 Sim MJW, Lu J, Spencer M, *et al*. High-affinity oligoclonal TCRs define effective adoptive T cell therapy targeting mutant KRAS-G12D. *Proc Natl Acad Sci U S A* 2020;117:12826–35.
52 Johnson LA, Morgan RA, Dudley ME, *et al*. Gene therapy with human and mouse T-cell receptors mediates cancer regression and targets normal tissues expressing cognate antigen. *Blood* 2009;114:535–46.
53 Morgan RA, Chinnasamy N, Abate-Daga D, *et al*. Cancer regression and neurological toxicity following anti-MAGE-A3 TCR gene therapy. *J Immunother* 2013;36:133–51.
54 Rohaan MW, Gomez-Eerland R, van den Berg JH, *et al*. MART-1 TCR gene-modified peripheral blood T cells for the treatment of metastatic melanoma: a phase I/IIa clinical trial. *Immunooncol Technol* 2022;15:100089.